Nonlinear Optimization Method for PGC Demodulation of Interferometric Fiber-Optic Hydrophone

Jiajing Wang(✉), Zhu Kou, and Xiangtao Zhao

Dalian Naval Academy, Dalian 116018, China
601770950@qq.com

Abstract. The fiber-optic hydrophone is an advanced detection method for modern naval anti-submarine warfare and underwater weapon testing, mainly used to detect marine acoustic environments. The phase generated carrier (PGC) demodulation technology is widely applied in interferometric fiber-optic hydrophones because of its wide dynamic range, high sensitivity, and high phase measurement accuracy. An ellipse fitting optimization method based on least squares is proposed in this paper to solve the nonlinear error in the PGC demodulation process to improve the system demodulation accuracy. The experimental results show that compared with the previous demodulation, after using the least-squares ellipse fitting optimization, the relative amplitude and harmonic suppression ratio of the same frequency are greatly improved, and the demodulation accuracy is effectively enhanced.

Keywords: Fiber-optic hydrophone · PGC demodulation · Nonlinear optimization · Ellipse fitting

1 Introduction

The phase generated carrier (PGC) demodulation technology realizes the demodulation due to the phase difference caused by changing two channels of optical signals. The commonly used methods include differential cross multiplication (PGC-DCM) [1] and arctangent (PGC-Arctan) algorithm. The method of arctangent algorithm is used in our paper. The previous PGC-Arctan demodulation algorithm is still affected by the modulation depth. When the modulation depth fluctuates, the demodulation result will produce nonlinearity and cause severe harmonic distortion [2]. The traditional PGC-Arctan algorithm also does not consider the accompanying amplitude modulation and system noise caused by the internal modulation. Moreover, the two demodulated signals contain non-orthogonal nonlinear errors. The graph that is drawn by the discrete points of the two signal outputs changes from a circle to an ellipse. This paper proposes a nonlinear optimization method of ellipse fitting based on least squares as a result. By means of the nonlinear optimization algorithm of least squares, the corresponding ellipse parameters are fitted. Then the orthogonal data after nonlinear optimization is demodulated

C. Yu et al. (Eds.): GPC 2022, LNCS 13744, pp. 162–168, 2023.
https://doi.org/10.1007/978-3-031-26118-3_12

by the PGC-Arctan algorithm, which can figure out the problem of spurious amplitude modulation. By comparing the direct way of demodulation and the least squares algorithm, the effectiveness of the proposed method for nonlinear error correction in the PGC demodulation process is verified.

2 Theory

This paper adopts the Mach-Zehnder interferometric fiber-optic hydrophone. There are two PGC modulation ways, including internal and external modulations. The light intensity expression of the interference output signal channel obtained by internal modulation is as follows:

$$S = (1 + m\cos\omega_0 t)(A + B\cos[C\cos\omega_0 t + \varphi(t)]) \tag{1}$$

where T and U are constants, which are directly proportional to the power of the light source, $Ccos\omega_0 t$ is a frequency-doubled carrier signal, and $\kappa(t)$ is the phase changes caused by the changes in external physical quantities [3]. The term $(1 + mcos\omega_0 t)$ is caused by the parasitic amplitude modulation, and m is the associated amplitude modulation index. At this time, the outputs of the two filters are:

$$S_1 = \frac{\mathrm{Tm}}{2} + \frac{Um}{2}[J_0(C) - J_2(C)]\cos\kappa(t) - UGJ_1(C)\sin\kappa(t) \tag{2}$$

$$S_2 = \frac{Um}{2}[J_3(C) - J_1(C)]\sin\kappa(t) - UGJ_2(C)\sin\kappa(t) \tag{3}$$

In Eqs. (2) and (3), $J_i(C)$ is the Bessel's functions of the i order. G is the amplitude value. Then the output of the ratio of S_1 to S_2 is no longer linear, and the traditional PGC-Arctan demodulation scheme is not applicable. Therefore, this paper proposes an ellipse fitting algorithm based on least-squares to solve the problem of the nonlinear error caused by associated amplitude modulation. On Account of the PGC-Arctan demodulation method, two-way orthogonal signals is obtained by ellipse fitting and the least-square nonlinear optimization on the two of low-pass filtered signals. The principle block scheme of the algorithm is shown in Fig. 1.

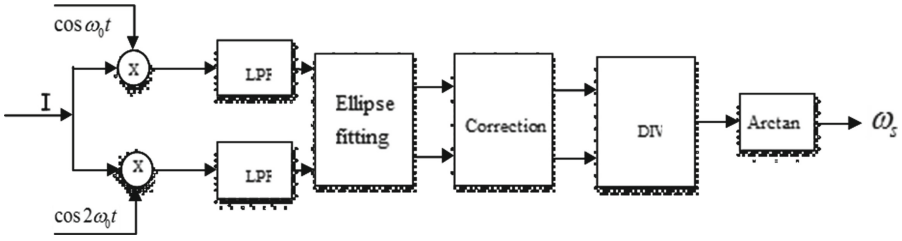

Fig. 1. The PGC demodulation method proposed in this paper.

The following part is the specific implementation of the algorithm. The final general expressions of the nonlinear error can be obtained by trigonometric transform on Eqs. (2)

and (3), which are as follows:

$$\begin{aligned} S_x &= h + t\cos[\kappa(t)] \\ S_y &= k + u\cos[\kappa(t) - \delta] \end{aligned} \tag{4}$$

In Eq. (4), S_x and S_y are the two channels of observed signals, and the nonlinear error in the equation is calibrated by an ellipse fitting algorithm to achieve the following expression:

$$\begin{aligned} S_x &= \cos[\kappa(t)] \\ S_y &= \sin[\kappa(t)] \end{aligned} \tag{5}$$

Equation (5) can be organized to:

$$\frac{(S_x - h)^2}{t^2} + \frac{(S_y - k)^2}{u^2} - 2\cos\delta(S_x - h)(S_y - k) \Big/ tu = \sin^2\delta \tag{6}$$

The known standard ellipse equation is shown below:

$$x^2 + Uxy + Cy^2 + Dx + Ey + F = 0 \tag{7}$$

The parameters h, k, t, u, and δ can be obtained by comparing Eq. (6) and Eq. (7), as shown in Eq. (8):

$$\begin{cases} h = (2CD - UE) \Big/ \left(U^2 - 4C\right) \\ k = (2E - UD) \Big/ \left(U^2 - 4C\right) \\ t = \left[\left(h^2 + k^2C + hkU - F\right) \Big/ \left(1 - U^2 \Big/ 4C\right)\right]^2 \\ u = \left(t^2 \Big/ C\right)^{\frac{1}{2}} \\ \delta = \cos^{-1}\left[-U \Big/ 2\sqrt{C}\right] \end{cases} \tag{8}$$

The parameters that the ellipse fitting calibration algorithm needs to calculate are the ellipse parameters U, C, D, E, and F [4]. This paper obtains the data $M = \{S_x; S_y\}_n$ through measurement. Then n groups of ellipse equations can be obtained by substituting them into Eq. (7), and the ellipse parameters U, C, D, E, and F can be obtained by using the least-squares method to optimize these n groups of equations. The residual can be acquired by substituting the data points $\{S_x; S_y\}$ into the ellipse equation, which is as follows:

$$S_{xi}^2 + US_{xi}S_{yi} + CS_{yi}^2 + DS_{xi} + ES_{yi} + F = r_i \tag{9}$$

Using the nonlinear optimization principle of the method of least-squares, the residual sum of the squares is calculated as:

$$P = \sum_{i=1}^{n} r_i^2 \tag{10}$$

To obtain the ellipse parameters that are infinitely close to the observed values, the minimum value of Eq. (10) is taken. Thus, the following equation should be satisfied:

$$\left.\frac{\partial P}{\partial u_i}\right|_{i=1}^{5} = 0, \quad u_i = U, C, D, E, F \tag{11}$$

Equation (11) is expanded to:

$$\begin{bmatrix} U \\ C \\ D \\ E \\ F \end{bmatrix} = \begin{bmatrix} \sum_{i=1}^{N} Sx_i^2 Iy_i^2 & \sum_{i=1}^{N} Sy_i^3 Ix_i & \sum_{i=1}^{N} Sx_i^2 Iy_i & \sum_{i=1}^{N} Sx_i Iy_i^2 & \sum_{i=1}^{N} Sx_i Iy_i \\ \sum_{i=1}^{N} Sy_i^3 Sx_i & \sum_{i=1}^{N} Sy_i^4 & \sum_{i=1}^{N} Sx_i Iy_i^2 & \sum_{i=1}^{N} Sy_i^3 & \sum_{i=1}^{N} Sy_i^2 \\ \sum_{i=1}^{N} Sx_i^2 Sy_i & \sum_{i=1}^{N} Sx_i Sy_i^2 & \sum_{i=1}^{N} Sx_i^2 & \sum_{i=1}^{N} Sx_i Sy_i & \sum_{i=1}^{N} Sx_i \\ \sum_{i=1}^{N} Sx_i Sy_i^2 & \sum_{i=1}^{N} Sx_i Sy_i^2 & \sum_{i=1}^{N} Sx_i Sy_i^2 & \sum_{i=1}^{N} Sy_i^2 & \sum_{i=1}^{N} Sy_i \\ \sum_{i=1}^{N} Sx_i Sy_i & \sum_{i=1}^{N} Sy_i^2 & \sum_{i=1}^{N} Sx_i & \sum_{i=1}^{N} Sy_i & N \end{bmatrix}^{-1} (-\begin{bmatrix} \sum_{i=1}^{N} Sx_i^3 Sy_i \\ \sum_{i=1}^{N} Sx_i^2 Sy_i^2 \\ \sum_{i=1}^{N} Sx_i^3 \\ \sum_{i=1}^{N} Sx_i^2 Sy_i \\ \sum_{i=1}^{N} Sx_i^2 \end{bmatrix}) \tag{12}$$

The ellipse parameters U, C, D, E, and F, obtained from Eq. (12), are substituted into Eq. (8) to calculate the parameters h, k, t, u, and δ. Then, by replacing the parameters h, k, t, u, and δ into Eq. (4), the interference signal after calibration can be achieved as shown in Eq. (13):

$$\begin{cases} S_x^{'} = (S_x - h)/t = \cos[\kappa(t)] \\ S_y^{'} = \dfrac{\left[(S_y - k)/u - \cos\kappa(t)\cos\delta\right]}{\sin\delta} = \sin[\kappa(t)] \end{cases} \tag{13}$$

where the data points $\{S'_x; I'_y\}$ are the two calibrated orthogonal interference signals.

3 Simulation

In order to analyze and verify the proposed method, relevant numerical simulations are carried out.

3.1 Simulation and Discussion of Associated Amplitude Modulation Index M

In this paper, the associated amplitude modulation index m is simulated from 0 to 0.3 by stepping of 0.05. Then, the output data before and after ellipse fitting are compared to determine whether the ellipse fitting algorithm on account of the least-squares can calibrate the nonlinear error caused by the associated amplitude modulation, and its optimization effect is verified. Figure 2 shows the variation results of the relative amplitude difference RAE, the harmonic suppression ratio HSR and the phase noise with the associated amplitude modulation index m.

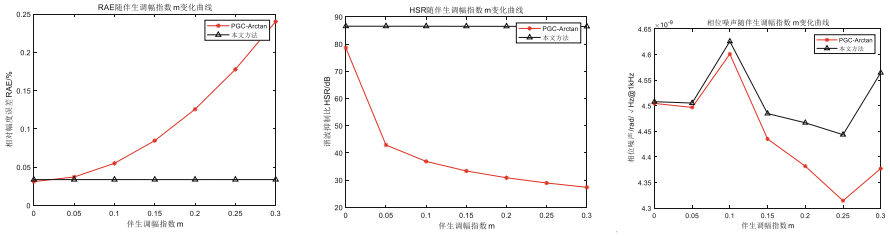

(a) (b) (c)

Fig. 2. Influence of the associated amplitude modulation index m on demodulation: (a) variation curve of RAE with m, (b) variation curve of HSR with m, and (c) variation curve of phase noise with m.

As shown in Fig. 2, with the increase in the parasitic amplitude modulation index, the RAE and HSR of the proposed method are basically stable at 0.03% and −87 dB, respectively, which meets the requirements of the index. However, the performance of the PGC-Arctan demodulation deteriorates sharply with the increase in the associated amplitude modulation, and the HSR even drops by 30 dB, so the demodulation function cannot be realized. In Fig. 2(c), with the increase in the parasitic amplitude modulation index m, the phase noises of the two algorithms have a slight change, both of which are less than 3×10^{-8} rad/Hz@1 kHz. However, the phase noise of the method in this paper is always higher than the PGC-Arctan demodulation, indicating that with the increase in the associated amplitude modulation index, the proposed method will increase the noise of some frequency points in the range of 1 kHz. However, this defect is negligible due to its relatively small value.

3.2 Simulation and Discussion of Two-Channel Signal Carrier Amplitude Ratio Gp/Hp

In this paper, the two-channel signal carrier amplitude ratio G_p/H_p is simulated from 1 to 10 by stepping of 1, and the output data before and after ellipse fitting are compared to determine whether the ellipse fitting algorithm on account of the least-squares can calibrate the nonlinear error caused by the amplitude deviation degree of the two-channel carriers, and its optimization effect is verified. Figure 3 shows the variation results of RAE, HSR, and phase noise with the carrier amplitude ratio G_p/H_p of the two signals.

In Fig. 3(a) and (b), with the increase in the amplitude ratio of the two signals, the RAE of the proposed technique is basically stable at 0.001%, and the HSR is stable at −87 dB, which fully meets the index requirements. However, the performance of PGC-Arctan demodulation deteriorates with the increase in the amplitude ratio of the two signals, and the demodulation function cannot be realized. As can be seen in Fig. 3(c), with the increase in the amplitude ratio of the two signals, the phase noise of the method in this paper is basically unchanged and less than 3×10^{-8} rad/Hz@1 kHz. However, the phase noise of the PGC-Arctan demodulation has always been growing with the maximum value exceeding 1.8×10^{-8} rad/Hz@1 kHz, indicating that with the increase in the amplitude ratio of the two signals, the method in this paper can effectively reduce the phase noise power and realize the optimization of nonlinear data.

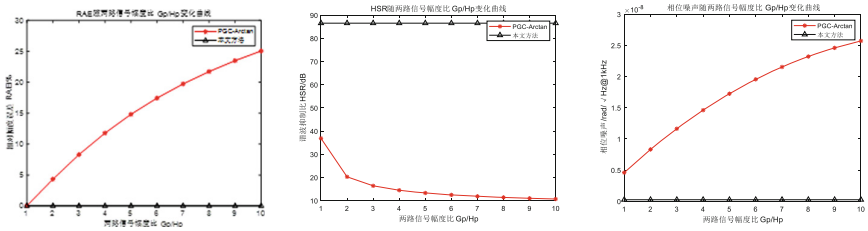

(a) (b) (c)

Fig. 3. Influence of two-channel signal carrier amplitude ratio G_p/H_p. On demodulation: (a) variation curve of RAE with G_p/H_p, (b) variation curve of HSR with G_p/H_p, and (c) variation curve of phase noise with G_p/H_p.

3.3 Simulation and Discussion of the Phase Difference K Between the Local Carrier and the Phase Carrier

In this paper, the phase shift K of the local carrier and the phase carrier is simulated from 0 to $\pi/4$ by stepping of $\pi/32$. The output data before and after ellipse fitting are compared to determine whether the ellipse fitting algorithm on account of the least-squares can calibrate the nonlinear error caused by the conversion of phase between the local carrier and the phase carrier, and its optimization effect is verified. Figure 4 shows the variation results of RAE, HSR, and phase noise with the phase shift K between the local carrier and the phase carrier.

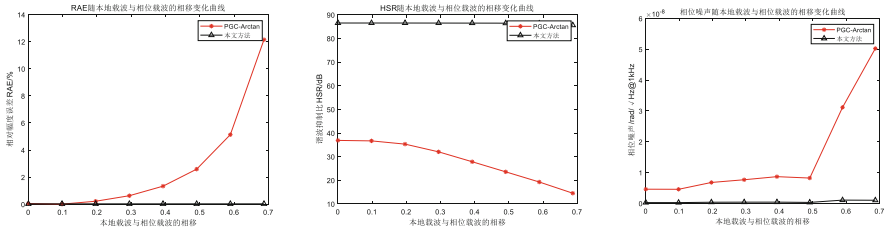

(a) (b) (c)

Fig. 4. Influence of the phase shift K between the local carrier and the phase carrier on demodulation: (a) variation curve of RAE with K, (b) variation curve of HSR with K, and (c) variation curve of phase noise with K.

It can be seen from Figs. 4(a) and (b) that with the increase in the conversion of phase between the local carrier and the phase carrier, the RAE of the proposed method is basically stable at 0.001%, and the total harmonic distortion is stable at −87 dB, which fully meets the requirements of the index. However, the performance of PGC-Arctan demodulation deteriorates sharply with the increase in the phase shift between the local carrier and the phase carrier, and the RAE exceeds 0.2%. Hence, the demodulation function cannot be realized. As can be seen from Fig. 4(c), with the increase of the phase shift between the local carrier and the phase carrier, the phase noise of both demodulations has some deterioration. When the phase shift is less than $5/32\pi$, the

phase noise of both methods is very small. When the phase shift is less than $5/32\pi$, the proposed method in this paper is clearly better than the PGC-Arctan demodulation, which proves that the proposed approach can effectively suppress the phase noise.

4 Conclusions

Aiming at the fluctuation of modulation depth in PGC demodulation and the associated amplitude modulation caused by internal modulation, this paper proposed an ellipse fitting method based on the least-squares and the traditional PGC-Arctan demodulation method to optimize the nonlinear error. Besides, three groups of data simulations compared the proposed method with the PGC-Arctan demodulation method. The conclusions are: (1) With the increase in the associated amplitude modulation index, the method in this paper performs well in various indicators. It can effectively solve the problem of the nonlinear error caused by the associated amplitude modulation. (2) With the increase in the amplitude ratio of the two signals, the method in this paper can effectively reduce the phase noise power and realize the optimization for the nonlinear data. (3) Considering that the signal in the actual environment of the military field usually contains ocean and polarization noises, the proposed method can eliminate the influence caused by noises. (4) When the relevant parameters fluctuate, the presented method can correctly calibrate the relevant parameters with relatively good stability and effectively reduce the amplitude distortion.

In summary, the method proposed in this paper can effectively calibrate the non-orthogonal data and realize the nonlinear optimization, which helps to improve the PGC demodulation performance of the fiber-optic hydrophones.

References

1. Han, C., Cao, J., Liu, X.: Research on the frequency characteristic of LPF in fiber-optic hydrophone system with PGC demodulation. Appl. Sci. Technol. **35**(5), 23–27 (2018)
2. Zhang, A., Wang, K., He, B.: Research on PGC demodulation algorithm of interference fiber sensor. Electro-Optic Tech. Appl. **28**(6), 49–53 (2013)
3. Cai, H., Ye, Q., Wang, Z.: Progress in research of distributed fiber acoustic sensing techniques. J. Appl. Sci. **36**(1), 41–58 (2018)
4. Shi, Q.: The stability and consistency analysis of optical seismometer system using phase generated carrier in field application. In: The International Society for Optical Engineering, pp. 75081M–75081M-9. Proceedings of SPIE, Shanghai (2009)